Biases in statistical inference: measles as a case study

Alexander Becker[4], Aaron A. King[1,2,3,*]
1 Department of Ecology & Evolutionary Biology, University of Michigan, Ann Arbor, Michigan, USA
2 Center for the Study of Complex Systems, University of Michigan, Ann Arbor, Michigan, USA
3 Department of Mathematics, University of Michigan, Ann Arbor, Michigan, USA
4 Courant Institute, New York University, New York, New York, USA
∗ E-mail: kingaa@umich.edu

Abstract

Important infectious disease parameters such as the basic reproductive ratio, R_0, and the infectious period are often estimated from long time series data by statistical inference. These estimated parameters have implications for how many doses of vaccine will be administered, how serious the outbreak will be, and how many people will be infected. However it is unclear how the underlying biological structures not explicitly included the mathematical model effect these estimates. We conduct a novel simulation study that investigates how biases in a mathematical model can lead to over estimation. We find that the bias introduced by under-reporting is insignificant, but the bias introduced by age structure results in over estimations in R_0 and the infectious period. These findings add another perspective to the field of statistical inference for disease models and suggests future work should focus on capturing these heterogeneities in simple models.

1 Introduction

As the field of infectious diseases increasingly becomes more mathematical, researchers look for ways to use various types of models to both explain biology and make predictions (Fraser et al. 2004; Hethcote 2000). The structure of these models vary greatly, from ordinary, partial, and stochastic differential equations (Keeling and Rohani 2007). However, the need for accurate parameter values is constant between them. In general, parameters such as the basic reproductive ratio, R_0, the infectious period, $\frac{1}{\gamma}$, and the transmission rate, β, are of particular importance to biologists, epidemiologists, and policy decisions (Lessler et al. 2011; May et al. 2001). These parameters are often extracted from time series data sets, and even though these time series can be as fine as weekly data for 20 years, factors such as under-reporting and age structure are frequently unknown in the data and subsequently not included in models. Under-reporting is difficult to extract and estimate from the data due to its relatively random nature. Additionally, under-reporting may vary with spatial location. Age structure also presents a difficulty as the age of first infection varies in urban versus rural populations (Singh and Datta 1997). This type of discrepancy may change estimates of the force of infection and is challenging to parametrize

in a model.

For example, the measles virus has been studied extensively and there exists long time series data (World Health Organization 2014), multiple mathematical models (Alexander et al. 2006; Bolker 1993; MacIntyre et al. 2002), and the disease itself often exhibits regular seasonal outbreaks. Outside of a large scientific literature, measles is still responsible for 164,000 deaths worldwide, although widely eradicated in the first world (Centers for Disease Control and Prevention 2013). Additionally parameter estimates on measles time series data displays interesting deviations. While currently accepted parameter values are R_0=7-17 (Wallinga et al. 2001), $\beta = 100 - 400$ per year, and $\frac{1}{\gamma}$=2 weeks, some studies have found significantly higher values, including an R_0 range of $30 - 57$ (He et al. 2010; Hooker et al. 2011; O. Bjornstad 2002). Although these high estimates may support a legitimate feature of the biology, a question to be asked is how do unobserved characteristics in the time series data manifest in the parameter estimates?

In general, the data for infectious disease incidence is skewed by under-reporting (Mette et al. 2011), and measles is no exception. The extent of under-reporting for measles ranges drastically from a 1.26:1 ratio in Germany (Mette et al. 2011), to a 2.5:1 ratio in Italy (Filia et al. 2013), up to a 22:1 ratio again in Italy (Ciofi Degli Atti et al. 2002), all the way up to 44 times higher in Switzerland (Richard et al. 2008). Possible reasons for under-reporting range from viewing the task as not important and a violation of privacy, to simply not knowing the reporting laws and procedure (Hume 1980; Konowitz et al. 1984). Under-reporting for measles is a continued problem (Filia et al. 2013), however it is not known how inference techniques are effected by this.

Although there exists data on infections per age (Singh and Datta 1997), and age structure models of both pre- and post- vaccine era (Schenzle 1984) exist, it is unclear how discrete age data effects parameter estimates. For example, measles is typically effects children under five and is spread through direct contact, making the force of infection age dependent (McLean and Anderson 1988), something that is not captured in the well mixed models.

With these questions in mind, we propose a simulation study following the same approach as He et al. (He et al. 2010) in both our use of measles as a case study and our implementation of iterated filtering techniques.

2 Methods and Models

Suppose we have a state process, X_t, an observation process, Y_t where observations are made at times $t_1, ..., t_N$, and a likelihood function $f(Y_{1:t_N}|\theta) = \Pi_{t=1}^{t_N} f(Y_t|Y_{t:t-1}, \theta)$ where θ is the parameter vector. From here, we can implement iterated filtering. Iterated filtering is a method to maximize the likelihood function via letting the parameters take a random walk in time developed by Ionides et al. (Ionides et al. 2006). In general, the MIF algorithm works by first selecting a starting parameter estimate $\hat{\theta}$, selecting a cooling fraction, an initial variance multiplier, and the number of iterations and then slowing "squeezing" $\hat{\theta}$ through parameter space and taking

the final iteration to be the maximum likelihood estimate (Ionides et al. 2006). This is a general overview, and the specific algorithm, development, and convergence criterion and properties can be found in (Ionides et al. 2011, 2006). A particularly important property is the *plug and play* property, i.e. the data can be simulated without the need to know explicit transition properties between states (Bret et al. 2009). These algorithms are implemented in the R package `POMP` (Partially Observed Markov Process) by King et al. (King et al. 2014). All simulations are run in the R programming language (R Core Team 2014).

In light of our original question – how do biases in the reported data effect the parameter estimates – we use simulated data. Our general procedure is to create 40-80 years of simulated data using an SIR model, keep only the reported cases class, and then use iterated filtering to estimate parameters from only the last 20 years of simulated data using the basic SIR model outlined in Figure 1. Using only a subset of the data allows us to capture the infection once it has gotten into a cycle to avoid transient effects. This general formulation has the advantage of being able to treat the time series as if it were "real" data while being able to see the true parameter values, which can be seen in Table 1. We use two models to produce data – a heterogeneous 30 compartment age structure model where transmission rate is based on contact rate per compartment, and a basic no age structure SIR model, which we call "well mixed". For the basic well mixed model, we assume mass action, stochastic, seasonal transmission, i.e. $\lambda = \beta \frac{I+\iota}{N} \frac{dW}{dt}(1 + 0.1 \sin 2\pi t)$. Additionally for both models we specify a measurement model, and the measurement model probability density function as required by the `POMP` package (King et al. 2014). We use the following SIR model to produce the data for the 30 age groups.

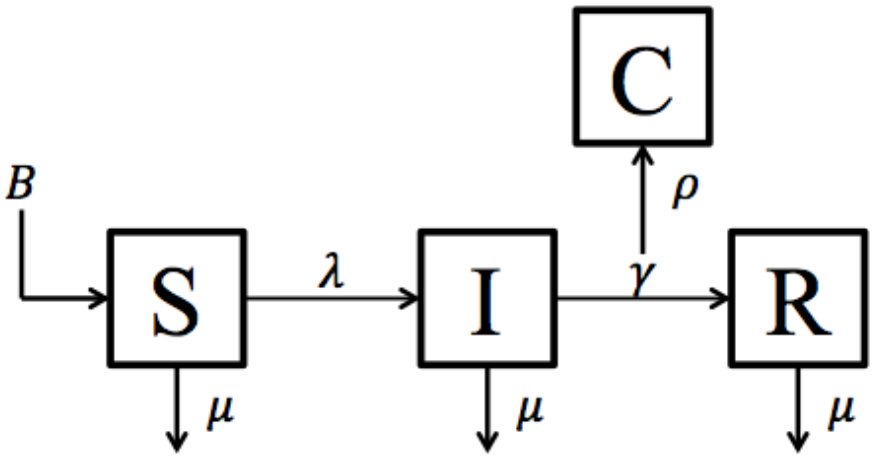

Figure 1: SIR flow diagram.

Parameter	Input Values	Description	Units
$\bar{\beta}$	140	transmission rate for age model	1/yr
b_0	140	transmission rate for well mixed model	1/yr
b_1	0.1	seasonality scaling	—
$\beta_{i,j}$	see text	transmission rate for each age compartment	—
θ	0-1	mixing parameter	—
μ	1/70	death rate	1/yr
B	1/70	birth rate	1/yr
γ	14	recovery rate	1/yr
ρ	$0.1 - 1$	reporting rate	—
R_0	10	basic reproductive rate	—
ι	2-3	visiting infected	—
N	10^6	number of individuals in the population	—
σ	0.05-0.15	white noise intensity	—
Nmif	50-200	number of `MIF` iterations	—
Nparticle	500-10^4	number of particles used for `MIF`	—

Table 1: Description and value of the parameters that we plug into the model to produce the simulated data.

$$\frac{dS_i}{dt} = -\sum_j \beta_{ij} \frac{I_j + \iota}{N_j} S_i \frac{dW}{dt}$$
$$\frac{dI_i}{dt} = \sum_j \beta_{ij} \frac{I_j + \iota}{N_j} S_i \frac{dW}{dt} - \gamma I_i$$
$$\frac{dR_i}{dt} = \gamma I_i$$
$$\frac{d\text{Incid}_i}{dt} = \gamma I_i \quad \text{for } i = 1, 2, ..., 30$$
$$\beta_{i,j} = \bar{\beta} f(\theta)(1 - \theta + \theta M_{i,j})(1 + 0.1 \sin(2\pi t))$$

We generate the cases data from a binomial draw of the sum of the incidence data with reporting probability ρ and the white noise parameter $\frac{dW}{dt}$ is drawn from a gamma distribution with intensity σ.

For the 30 compartment model, we have population age classes, 0, 1,..., 19, 20-25,..., 60-65, 65+. We begin with an population distribution of an equal number in each compartment multiplied by how long one remains in that compartment. The initial conditions of S_i and I_i begin at a steady state value, with $S_i = \frac{BN}{10}$ and $I_i = B^2 N \gamma$ where each is multiplied by how long one remain in that compartment. For both the age structure model and the well-mixed model parameter estimations we use the true S, I, R values as our initial conditions to avoid transient effects.

As we want to look at how age structure effects parameter estimates, we need to choose $\beta_{i,j}$

such that as we vary θ, which corresponds to different levels of heterogeneity, we keep a fixed R_0. For instance, $\theta = 1$ corresponds to $\beta_{i,j}(1) = \bar{\beta}(M_{i,j})$ which is a completely heterogeneous matrix. On the other hand, $\theta = 0$ corresponds to $\beta_{i,j}(0) = \bar{\beta}$ which is a completely homogeneous matrix. This comes down to providing a scaling factor $f(\theta)$ in the next generation matrix $G_{i,j} = \frac{\bar{\beta}}{\mu+\gamma} f(\theta)(1 - \theta + \theta M_{i,j})$ where $M_{i,j} = C_{i,j}\frac{N_i}{N_j}$ where $C_{i,j}$ is the contact matrix provided by Mossong et al. (Mossong et al. 2008). As $R_0 = \rho(G)$, where ρ is the spectral radius, we get $f(\theta) = \rho(1-\theta+\theta M_{i,j})^{-1}$. This allows us to preserve $R_0 = \frac{\bar{\beta}}{\mu+\gamma}$ regardless of θ. This scaling also has the advantage of preserving the average number of contacts each age group has independent of θ. In the same way, for the basic SIR model we use the definition that $R_0 = \frac{\beta}{\gamma+\mu}$. As μ is on the order of 10^{-2}, we use the approximation $R_0 \approx \frac{\beta}{\gamma}$. Examples of the time series plots and scaled contact matrices for various levels of heterogeneity used can be seen in Figure 2. Note that for the contour plots in Figure 2, age versus age should be read as the amount of contact age group A has with age group B.

Note that regardless of the level of mixing, the time series data consists of yearly outbreaks. However, the well mixed, $\theta = 0$, data has consistent peaks, where as the heterogenous data, $\theta = 1$, hits higher peaks and lower valleys. In the contact matrix plots matrix plots for the heterogenous populations, contact within the age group is very common and corresponds to school age. Additionally note that the contact matrix is not symmetric. While a non symmetric contact is not immediately intuitive, an explanation is the example of a teacher having contact with multiple young students, but the students not being in contact with as many adults.

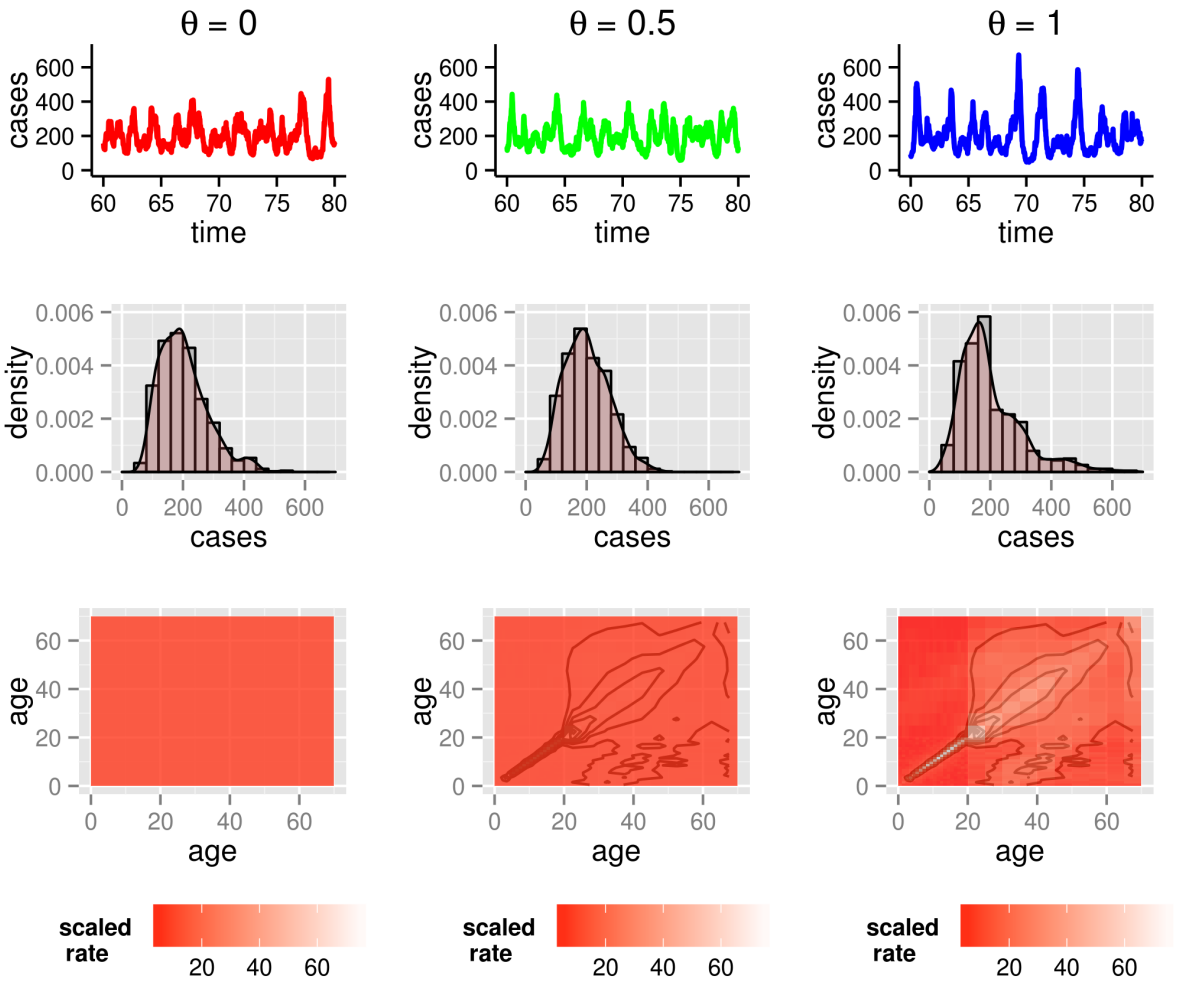

Figure 2: Simulated data for $\theta = 0, 0.5, 1$. Both the time series plots and the scaled contact matrix $\beta_{i,j}$.

We simulate aging, births, and deaths with the following scheme, where we evaluate this at every time step Δt. This scheme allows us to simulate entry, exit, and movement between compartments as a "trickle" process instead of a group movement process, i.e. not everyone will age by a year at identical times. Note that as in the well-mixed model, the population remains constant.

$$
\begin{aligned}
Q_i &= \begin{cases} Q_i + \Delta t(BN - Q_i - \mu Q_i) & \text{if } Q = S \\ Q_i + \Delta t(-Q_i - \mu Q_i) & \text{if } Q = I, R \end{cases} \quad \text{for age 0} \\
Q_i &= Q_i + \Delta t(Q_{i-1} - Q_i - \mu Q_i) \quad \text{for ages 1,..., 19} \\
Q_i &= Q_i + \Delta t\left(\frac{Q_{i-1}}{5} - \frac{Q_i}{5} - \mu Q_i\right) \quad \text{for ages 20-24, 25-29,..., 60-64} \\
Q_i &= Q_i + \Delta t\left(\frac{Q_{i-1}}{5} - \mu Q_i\right) \quad \text{for ages 65+} \\
Q &\in \{S, I, R\}
\end{aligned}
$$

Once we've produced the data from the 30 compartment model, we pool it together into single S, I, R, incidences, and cases compartments. From here, we use a standard SIR model with under-reporting to fit the generated data. We use the following numerical scheme to estimate parameters based only on the combined cases compartment from the age model. This scheme has the benefit of never allowing the populations to become negative while still being the first order method. Using the standard SIR finite different scheme gives the possibility of allowing certain compartments to become negative, thus making the binomial draw for cases result in a `NaN` value. This is especially problematic for parameter estimation where certain parameters may have to go through biologically unnatural regions of parameter space before settling to the true value.

$$
\begin{aligned}
S_{t+\Delta t} &= \exp(-\mu\Delta t)(BN\Delta t - S_t(1 - \exp(-\lambda_t \Delta t))) \\
I_{t+\Delta t} &= \exp(-\mu\Delta t)(S_t(1 - \exp(-\lambda_t \Delta t)) - I_t(1 - \exp(-\gamma\Delta t))) \\
R_{t+\Delta t} &= \exp(-\mu\Delta t)(I_t(1 - \exp(-\gamma\Delta t))) \\
\text{Incid}_{t+\Delta t} &= I_t(1 - \exp(-\gamma\Delta t)) \\
\text{Cases} &\sim \text{binomial}(\text{Incid}, \rho) \\
\lambda_t &= \beta \frac{dW}{dt} \frac{I_t + \iota}{N} \\
\beta &= b_0(1 + b_1 \sin 2\pi t)
\end{aligned}
$$

Additionally the parameters to be estimated, γ, β, ρ, are transformed to prevent them from entering regions of parameter space where they will attain non biologically accurate values. Parameters γ and β are log transformed while ρ is logit transformed.

As we want to estimate parameters we need to find the translation under this scheme. In continuous time, the infectious period is estimated as IP=$\frac{1}{\gamma}$. From here we know $\frac{T}{\Delta t} \sim$ geometric(p), therefore $\mathbb{E}(\frac{T}{\Delta t}) = \frac{1-p}{p}$ where $p = 1 - \exp(-\gamma\Delta t)$. Then $\mathbb{E}(T) = \frac{\Delta t}{\exp(\gamma\Delta t)-1} \sim \frac{1}{\gamma} + O(\Delta t)$. Therefore, for sufficiently small Δt, we can estimate our infectious period, IP, by $\frac{1}{\gamma}$.

3 Results

3.1 Under-Reporting

We begin by looking at the simplest case – under-reporting. We run the well mixed SIR model while varying the under-reporting rate ρ and produce a data set for each ρ. From here, we use iterated filtering to estimate b_0, γ, and thus R_0, as well as ρ. Note that $b_0 = \text{mean}(\beta)$ which we use as our estimate for β. The idea with this section is to see if simple changes in the actual reporting ratio will be enough to produce high estimates of other parameters, specifically R_0. The results are in Figure 3. In all plots the hat refers to the parameter estimate.

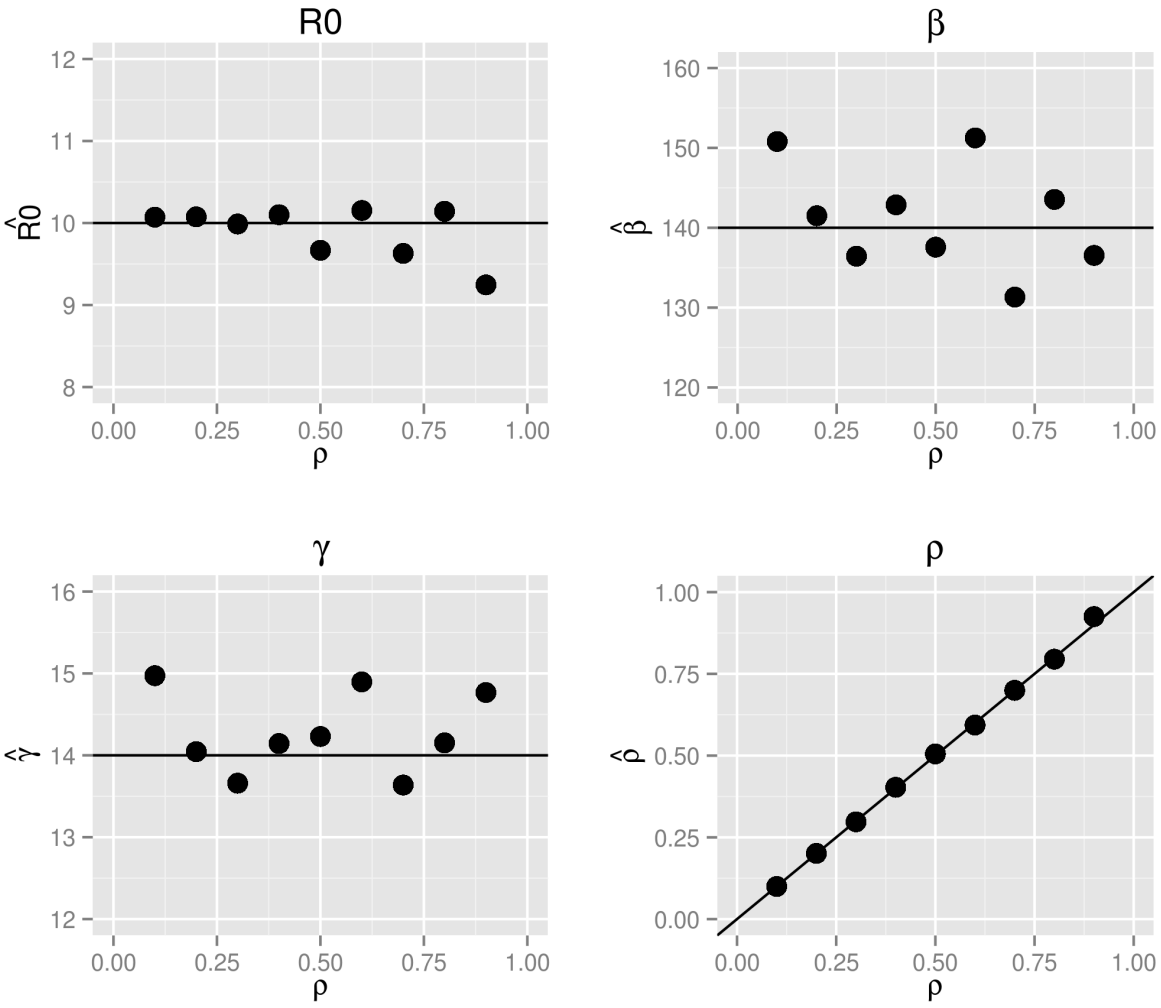

Figure 3: Results of estimating β, γ, ρ, and R_0 from simulated data for various values of ρ. The solid line represents the true input value for the parameter.

Note that in this data, whenever there is an over estimate or under estimate of β, γ will also be over estimated or under estimated in order to compensate, thus keeping R_0 estimates within $\pm$ of the true value. Additionally, parameter estimates for ρ are almost recovered exactly at every step. These results indicate that in a well mixed population, assuming other parameters such as birth and death rate are known, transmission and the infectious period can be recovered very close to their true value. Therefore, within a homogeneous population, under-reporting ρ causes almost no statistical bias, and R_0 and infectious parameters can be estimated within 10% of their original value.

3.2 Age Structure

Next we look at how age structure, specifically heterogeneities in the population effect our parameter estimates. As noted before, regardless of the level of transmission heterogeneity, R_0 remains fixed in the age structure model, as does reporting probability ρ. The results are in Figure 4

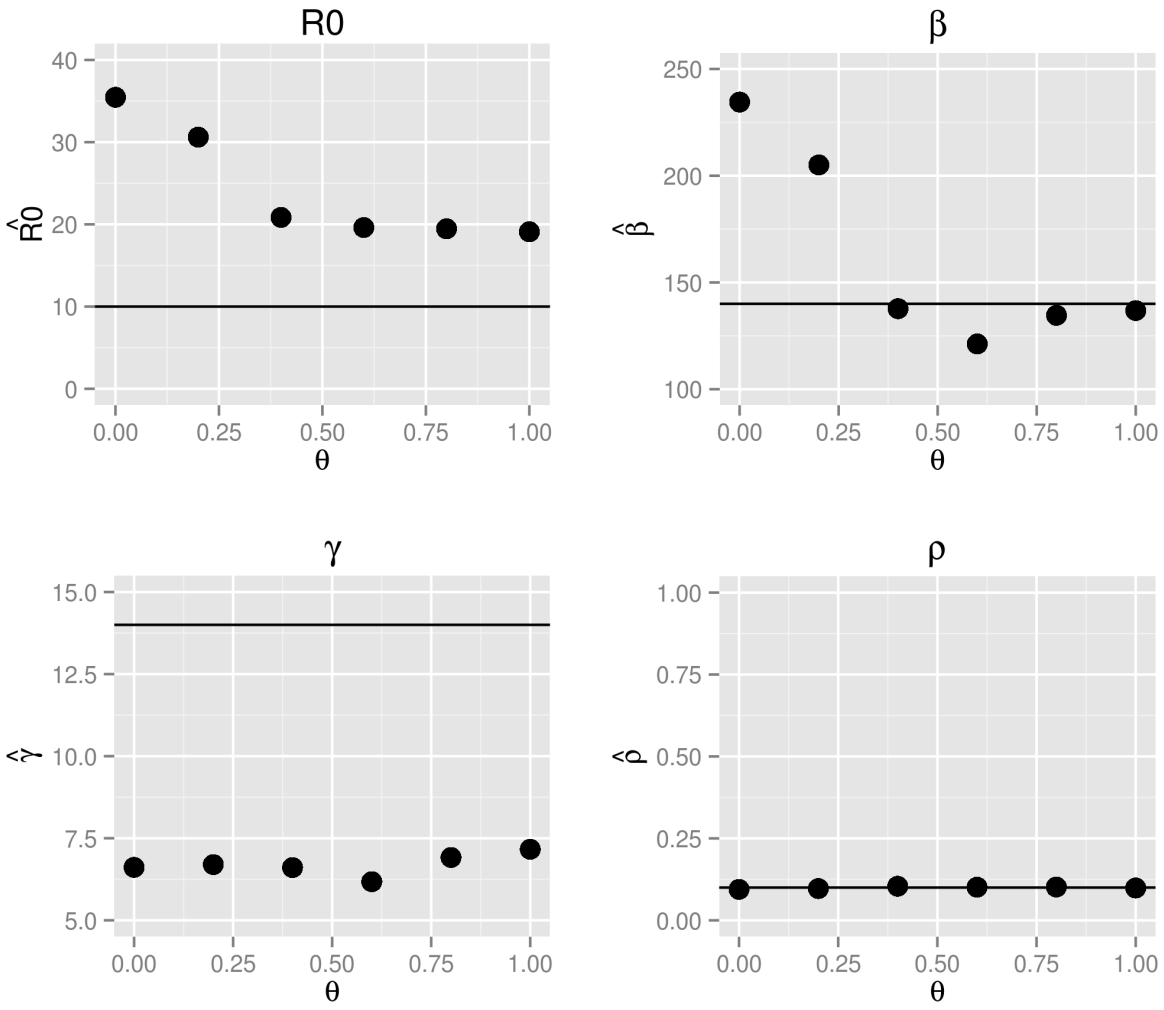

Figure 4: Results of estimating β, γ, ρ, and R_0 from simulated data for various values of mixing parameter θ. The solid line represents the true input value for the parameter.

As observed in Figure 4, ρ is always recovered which is consistent with the findings in Figure 3, and β is recovered for higher values of θ. However, R_0, and more specifically, γ is not recovered, with γ consistently halved. The estimate $\hat{\gamma} = \frac{1}{2}\gamma$ implies that the estimated infectious period will be twice the actual infectious period, even when beta is estimated to be the true value. This indicates that unlike the results in Figure 3, in an age structured setting, γ and β are unable to balance each other to preserve the true R_0 value. This also indicates that a simple SIR cannot be used to fit age partitioned data, even in the regime of quite low levels of heterogeneity in a population.

Additionally, these results show that even in the "test" case $\theta = 0$ where the age structured model should be equivalent to a partitioned well mixed model, biases still form and skew R_0 estimates. Additionally these biases propagate throughout the model for each value of θ resulting in R_0 two to almost four times higher than the input values. These results are consistent with the findings by (He et al. 2010; Hooker et al. 2011; O. Bjornstad 2002).

A typical convergence plot can be seen in Figure 5. These plots indicate that the values of actually converging and that likelihood is consistently maximized.

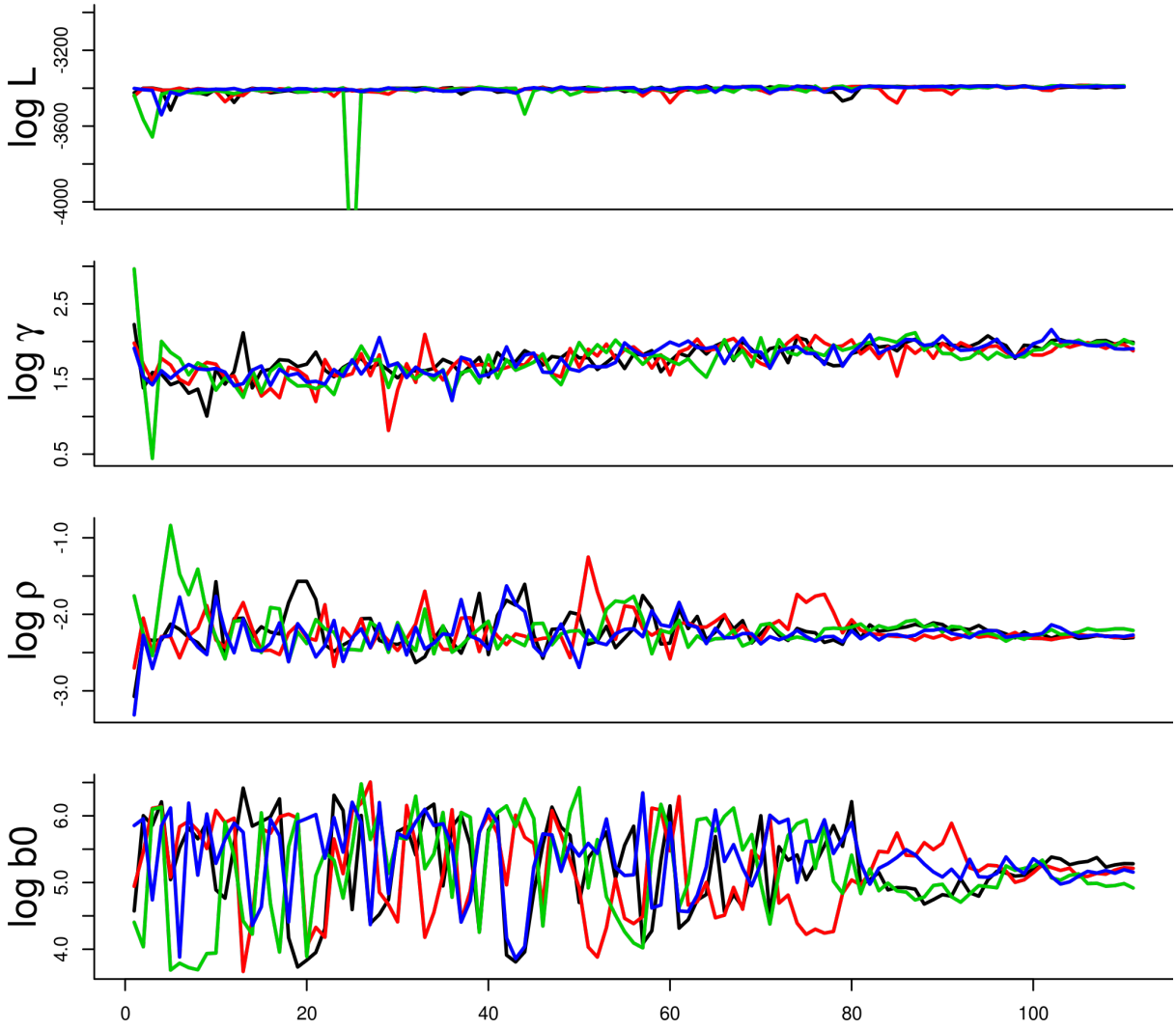

Figure 5: Iterated filtering convergence plots for $\theta = 1$, these are typical of each θ value.

Additionally, in the age structure model formulation, we have tried $\sum \frac{I_j}{N_j}$ and $\frac{1}{N}\sum I_j$ and ob-

serve the same biases in γ and R_0. Additionally, as seen in Figure 5, γ and ρ converge quickly, and while b_0 does not converge at the same speed, the final values are quite clustered. When the estimated parameters are plugged back into the well mixed model, we see similar behavior in the final 10 years of simulated data, as seen in Figure 6. Note that the relative error is generally small, however there is a large relative error spike that year 70, seemingly before the data syncs up to the true values.

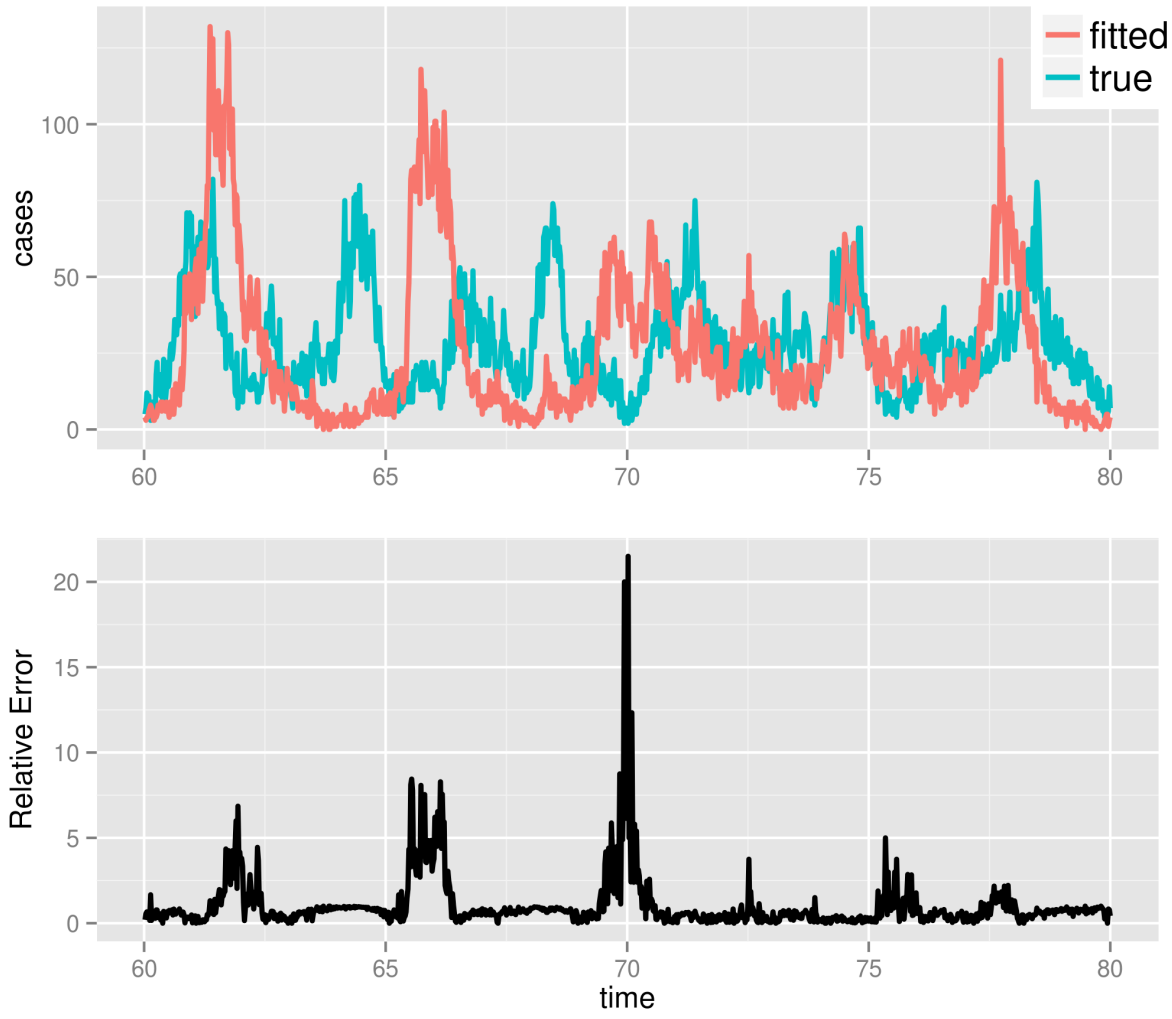

Figure 6: Simulated data (blue) and fitted data (red) for $\theta = 0$ as well as the relative error between the two plots.

These results indicate that not only does age heterogeneity result in high estimates of R_0 and the infectious period $\frac{1}{\gamma}$, but that the biases can form even in zero or low heterogeneous conditions.

4 Discussion

4.1 Conclusions

Currently, the World Health Organization (WHO) have stated two target goals – 1) reducing global measles mortality by 95% compared to 2000 estimates by 2015, and 2) eliminate measles in at least five WHO regions by 2020 (World Health Organization 2012).

We find that under-reporting alone is not responsible for the double or triple R_0 estimates seen in (He et al. 2010), but can be responsible for variations. However this is not surprising, as in theory reporting rate ρ is essentially a stochastic scaling factor.

However, in the age structure model we do find biases. While it is reasonable to assume that higher R_0 values could form for high levels of heterogeneity, it is not obvious that biases should for essentially a partitioned well mixed model. Possible reasons could be attributed to different sized compartments and thus the ageing rates.

These results overall show that while under-reporting does not effect parameter estimates in the simulated data, age structure has dramatic effects on γ, R_0, and in certain mixing regimes, β.

4.2 Limitations

On the technical side, particle filtering has many strengths, there are also some disadvantages – both expected and unexpected. It is a known fact that the codes are computationally expensive and each data set parameter estimation can take hours. Additionally, in the discrete time SIR model, our steady states are dependent on step size Δt, for example at steady state we have $I^* = \frac{\mu \Delta t}{1 - e^{(\mu+\gamma)\Delta t} - \frac{\mu}{\beta}}$. This puts an explicit limit on the required step size Δt.

4.3 Next Steps

Previous studies have suggested using a parameter α and a non-linear incidence function, $\lambda = \beta(\frac{I}{N})^\alpha$, to look at the level of inhomogeneity. However in an analysis of twenty data sets, this parameter was estimated to be $\alpha = 1$ He et al. (2010). Our results indicate that in a basic well-mixed SIR model, more work should be done to capture age heterogeneities.

Previous work has considered their transmission parameter β to be a function of the school term and the holiday reflecting increased transmission for children in school (He et al. 2010; Schenzle 1984). This formulation could be included in future age structure models.

Additionally our uniform treatment of age classes is not the most realistic approach. We assume that there are an equal number of people in each age group whereas finding the initial distribution using the McKendrick PDE in steady state, $n_t + n_a = -\mu n$ and therefore $N(a, a + \Delta a) = \frac{BN}{\mu} e^{-\mu a}(1 - e^{-\mu \Delta a})$, where N is the number of individuals per age group, may be more realistic (Hethcote 2000). We also assume that every age class dies at the same rate, whereas probability of dying may not be evenly distributed (McLean and Anderson 1988). In the same way, we assume that birth is a function of the entire population, whereas birth is really a function of a select number of age groups. However, as we are primarily investigating bias formation, these changes are not essential to our findings.

Finally, another potential bias is the spatial nature of epidemics, which should be also be investigated.

5 Acknowledgments

This project was supported by the University of Michigan Mathematics Research Experience for Undergraduates.

References

Alexander, M. E., S. M. Moghadas, P. Rohani, and A. R. Summers. 2006. Modelling the effect of a booster vaccination on disease epidemiology. Journal of Mathematical Biology, **52**:290–306.

Bolker, B. 1993. Chaos and complexity in measles models: a comparative numerical study. IMA journal of mathematics applied in medicine and biology, **10**:83–95.

Bret, C., D. He, E. L. Ionides, and A. A. King. 2009. Time series analysis via mechanistic models. The Annals of Applied Statistics, **3**:319–348.

Centers for Disease Control and Prevention. 2013. Measles: Overview of measles disease.

Ciofi Degli Atti, M. L., S. Salmaso, A. Bella, R. Arigliani, M. Gangemi, G. Chiamenti, G. Brusoni, A. E. Tozzi, and Pediatric Sentinel Surveillance Study Group. 2002. Pediatric sentinel surveillance of vaccine-preventable diseases in italy. The Pediatric infectious disease journal, **21**:763–768.

Filia, A., A. Bella, M. Rota, A. Tavilla, F. Magurano, M. Baggieri, L. Nicoletti, S. Iannazzo, M. Pompa, and S. Declich. 2013. Analysis of national measles surveillance data in italy from october 2010 to december 2011 and priorities for reaching the 2015 measles elimination goal. Euro surveillance: bulletin Europen sur les maladies transmissibles = European communicable disease bulletin, **18**.

Fraser, C., S. Riley, R. M. Anderson, and N. M. Ferguson. 2004. Factors that make an infectious disease outbreak controllable. Proceedings of the National Academy of Sciences of the United States of America, **101**:6146–6151.

He, D., E. L. Ionides, and A. A. King. 2010. Plug-and-play inference for disease dynamics: measles in large and small populations as a case study. Journal of The Royal Society Interface, **7**:271–283.

Hethcote, H. 2000. The mathematics of infectious diseases. SIAM Review, **42**:599–653.

Hooker, G., S. P. Ellner, L. D. V. Roditi, and D. J. D. Earn. 2011. Parameterizing state-space models for infectious disease dynamics by generalized profiling: measles in ontario. Journal of the Royal Society Interface, **8**:961–974.

Hume, J. C. 1980. On reports and rapport in VD control. American Journal of Public Health, **70**:946–947.

Ionides, E. L., A. Bhadra, Y. Atchad, and A. King. 2011. Iterated filtering. The Annals of Statistics, **39**:1776–1802.

Ionides, E. L., C. Bret, and A. A. King. 2006. Inference for nonlinear dynamical systems. Proceedings of the National Academy of Sciences, **103**:18438–18443.

Keeling, M. J. and P. Rohani. 2007. Modeling Infectious Diseases in Humans and Animals. Princeton University Press, Princeton, 1 edition.

King, A. A., E. L. Ionides, C. M. Bretó, S. Ellner, B. Kendall, H. Wearing, M. J. Ferrari, M. Lavine, and D. C. Reuman. 2014. pomp: Statistical inference for partially observed Markov processes (R package).

Konowitz, P. M., G. A. Petrossian, and D. N. Rose. 1984. The underreporting of disease and physicians' knowledge of reporting requirements. Public Health Reports, **99**:31–35.

Lessler, J., W. J. Moss, S. A. Lowther, and D. a. T. Cummings. 2011. Maintaining high rates of measles immunization in africa. Epidemiology & Infection, **139**:1039–1049.

MacIntyre, C. R., N. J. Gay, H. F. Gidding, B. P. Hull, G. L. Gilbert, and P. B. McIntyre. 2002. A mathematical model to measure the impact of the measles control campaign on the potential for measles transmission in australia. International journal of infectious diseases: IJID: official publication of the International Society for Infectious Diseases, **6**:277–282.

May, R. M., S. Gupta, and A. R. McLean. 2001. Infectious disease dynamics: what characterizes a successful invader? Philosophical Transactions of the Royal Society of London. Series B: Biological Sciences, **356**:901–910.

McLean, A. R. and R. M. Anderson. 1988. Measles in developing countries. part i. epidemiological parameters and patterns. Epidemiology and Infection, **100**:111–133.

Mette, A., A. M. Reuss, M. Feig, L. Kappelmayer, A. Siedler, T. Eckmanns, and G. Poggensee. 2011. Under-reporting of measles. Deutsches rzteblatt International, **108**:191–196.

Mossong, J., N. Hens, M. Jit, P. Beutels, K. Auranen, R. Mikolajczyk, M. Massari, S. Salmaso, G. S. Tomba, J. Wallinga, J. Heijne, M. Sadkowska-Todys, M. Rosinska, and W. J. Edmunds. 2008. Social contacts and mixing patterns relevant to the spread of infectious diseases. PLoS Med, **5**:e74.

O. Bjornstad, B. F. F. 2002. Dynamics of measles epidemics: Estimating scaling of transmission rates using a time series SIR model. **72**:169–184.

R Core Team. 2014. R: A Language and Environment for Statistical Computing. R Foundation for Statistical Computing, Vienna, Austria.

Richard, J.-L., B. Vidondo, and M. Mäusezahl. 2008. A 5-year comparison of performance of sentinel and mandatory notification surveillance systems for measles in switzerland. European Journal of Epidemiology, **23**:55–65.

Schenzle, D. 1984. An age-structured model of pre- and post-vaccination measles transmission. Mathematical Medicine and Biology, **1**:169–191.

Singh, J. and K. K. Datta. 1997. Epidemiological considerations of the age distribution of measles in india: a review. Journal of Tropical Pediatrics, **43**:111–115.

Wallinga, J., D. Lvy-Bruhl, N. J. Gay, and C. H. Wachmann. 2001. Estimation of measles reproduction ratios and prospects for elimination of measles by vaccination in some western european countries. Epidemiology and Infection, **127**:281–295.

World Health Organization. 2012. Global measles and rubella: Strategic plan 2012-2020.

World Health Organization. 2014. Measles reported cases.